



Behavior of Reinforced Concrete Continuous Beams under Pure Torsion

Saad Khalaf Mohaisen

Assistant Professor

College of Engineering

Al-Mustansiriya University

eng_saad@uomustansiriyah.edu.iq

Ali Adel Abdulhameed

Assistant Lecturer

Department of Engineering Affairs

University of Baghdad

aliadel@uobaghdad.edu.iq

Majid Mohammad Kharnoob

Lecturer

Department of Engineering Affairs

University of Baghdad

dr.majidkharnoob@uobaghdad.edu.iq

ABSTRACT

Practically, torsion is normally combined with flexure and shear actions. Even though, the behavior of reinforced concrete continuous beams under pure torsion is investigated in this study. It was performed on four RC continuous beams under pure torsion. In order to produce torsional moment on the external supports, an eccentric load was applied at various distances from the longitudinal axis of the RC beams until failure.

Variables considered in this study are absolute vertical displacement of the external supports, torsional moment's capacity, angle of twist and first cracks occurrences. According to experimental results; when load eccentricity increased from 30cm to 60cm, the absolute vertical displacement increased about 46.92% and the angle of twist increased about 45.76% at failure. It has been also found that the ultimate failure loads decreased about 49.65% when the load eccentricity increased from 30cm to 60cm. Furthermore, the first crack was monitored and it was found that the first crack occurred at higher stages of loading with low loading eccentricity. The first crack records appeared at 75.86%, 70.80%, 63.16% and 54.79% of loading when the load eccentricities are 30, 40, 50 and 60cm, respectively.

Key words: angle of twist, continuous beam, eccentric loading, pure torsion, torsional moments.

سلوك العتبات الخرسانية المسلحة والمستمرة تحت تأثير عزوم اللي الصرفة

ماجد محمد خرنوب

مدرس

قسم الشؤون الهندسية

جامعة بغداد

علي عادل عبد الحميد

مدرس مساعد

قسم الشؤون الهندسية

جامعة بغداد

سعد خلف محيسن

أستاذ مساعد

كلية الهندسة

الجامعة المستنصرية

الخلاصة

عملياً عزوم اللي عادةً ما تشترك مع عزوم الأحناء وقوى القص. على الرغم من ذلك، تمت دراسة سلوك العتبات الخرسانية المسلحة والمستمرة تحت تأثير عزوم اللي الصرفة في هذا البحث حيث تمت دراسة تصرف أربعة عتبات مسلحة ومستمرة تحت تأثير عزوم اللي. ولغرض الحصول على عزوم اللي على المساند الخارجية، تم تسليط أحمال لامركزية وعلى مسافات مختلفة من المحور الطولي للعتبات الخرسانية المسلحة والمستمرة حتى فشل العتبة.

تتضمن المتغيرات التي تم دراستها في هذا البحث دراسة الهطول النسبي للمساند الخارجية، سعة العتبات المستمرة لتحمل عزوم اللي، زاوية اللي وحدوث التصدع الأولي. أظهرت النتائج عند زيادة بعد القوى المسلطة عن المحور الطولي للعتبة من 30سم الى 60سم أنتج زيادة الهطول النسبي للمساند الخارجية بنسبة 46.92% وزيادة زاوية اللي بنسبة 45.76% عند الفشل. بينت النتائج العملية نقصان في قوى التحمل القصوى للعتبات الخرسانية المسلحة بنسبة 49.65% عند زيادة بعد القوى المسلطة عن المحور الطولي للعتبة من 30سم الى 60سم. أيضاً تم مراقبة التصدع الأولي للعتبات حيث حدث التصدع الأولي عند تسليط أحمال بنسبة



المحور الطولي للعتبات المستمرة وعلى الترتيب. 75.86%، 70.8%، 63.16%، 54.79% من الحمل الأقصى وحالات التحميل اللامركزي لمسافات 30، 40، 50، 60 سم من

1. INTRODUCTION

Appreciable torsion does occur in many structures, such as in the main girders of bridges which are twisted by transverse beams or slabs. It occurs in buildings where the edge of a floor slab and its beams are supported by a spandrel beam running between the exterior columns. This situation is illustrated in **Fig.1**, where the floor beams tend to twist the spandrel beam laterally.

In complex structures such as helical stairways, curved beams, and eccentrically loaded box beams, the torsional effects dominate the structural behavior. Torsional moment tends to twist the structural member around its longitudinal axis, inducing shear stresses. However, structural members are rarely subjected to pure torsional moment. In most cases, torsional moments act concurrently with bending moment and shear forces, **Mahmoud, and Basile, 2007**.

Earthquakes can cause dangerous torsional forces in all buildings. This is particularly true in asymmetrical structures, where the centers of mass and rigidity do not coincide. Other cases where torsion may be significant are in curved bridge girders, spiral stairways, and balcony girders, and whenever large loads are applied to any beam "off center", **McCormac, and Brown, 2014**.

It is important for designers to distinguish between two types of torsions: equilibrium torsion and compatibility torsion. Equilibrium torsion occurs when the torsional resistance is required to maintain static equilibrium. For this case, if sufficient torsional resistance is not provided, the structure will become unstable and collapse. External loads have no alternative load path and must be resisted by torsion, **Kamara, and Rabbat, 2005**.

Compatibility torsion develops where redistribution of torsional moments to adjacent members can occur. The term compatibility refers to the compatibility of deformation between adjacent parts of a structure, **Fanella, and Rabbat, 1997**.

Depending upon the nature of applied loading, structural form and position of the member under consideration in the structural system, the twisting moments may be static or dynamic, transient or sustained and non-repetitive or cyclic. Static torsion occurs when the loads are applied gradually at a slow rate so that the twisting moment increases monotonically from zero to its full value. In this case the, internal resisting torque at any stage is in equilibrium with the external applied torque. Most of the torsion tests on concrete members and structural systems reported in the last decades deal with monotonically increasing static torsion. Transient or short-term twisting moments arise due to temporary live loads and environmental effects such as wind and seismic forces. On the other hand long time torsion is produced by dead loads and live loads, which are more or less permanent, **Kumar, et al., 2015**.

Reinforced concrete continuous beams under pure torsion were seldom studied, so the main objectives of this study were to investigate the torsional behaviors of reinforced concrete continuous beams under pure torsion condition.



2. EXPERIMENTAL WORK

2.1 Materials

All materials used in this experimental study have been tested according to international and Iraqi specifications and as follows:

2.1.1 Cement

Al-Mass ordinary Portland cement Type I cement was used. The cement was tested and checked according to **IQS no.5, 1984**. The chemical and physical properties of used cement are shown in **Tables 1 and 2**, respectively.

2.1.2 Fine aggregate

AL-Ukhaider natural sand of 4.75 mm maximum size was used throughout this work. **Table 3** shows the grading of fine aggregate. Results showed that the fine aggregate grading and sulfate content were within the requirements of the **IQSno.45, 1984**. The specific gravity, sulfate content and absorption of fine aggregate are shown in **Table4**.

2.1.3 Coarse aggregate

Crushed gravel with maximum size of 20 mm from Al-Niba'ee region was used. The grading of coarse aggregate is given in **Table 5** which confirms to the **IQS no.45, 1984**. The physical properties of coarse aggregate are given in **Table6**.

2.1.4 Reinforcing steel

Deformed steel reinforcement of 10 mm diameter was used for the main reinforcement and steel bars of diameter 8 mm are used for stirrups. Test results refer that the adopted steel bars conformed to **ASTM A615M-01** as shown in **Table 7**. The bars have been tested in the material laboratory of the Civil Engineering Department at Al-Mustansiriyah University, Baghdad, Iraq.

2.1.5 Water

Tap water was used for both mixing and curing of concrete.

2.2 Mix Design

Several trial mixes were made according to the recommendations of the **ACI 211.1-91**. Reference concrete mixture was designed to achieve cube strength of 31 MPa at 28 days. The mixture was (1 cement: 1.5sand: 3 gravel, by weight), and the slump was approximately 100 mm. Mixture details are given in **Table8**. It was found that the used mixture produces good workability and uniform mixing of concrete without segregation and the resulted compressive strength (avg. of 3 cubes at each age) was 23.5 MPa and 31.5 MPa at 7 and 28 days age, respectively.

2.3 Test Beams Details

To study the most influential variables on torsional behavior of reinforced concrete continuous two-equal spans beams under pure torsion, four reinforced concrete beams were reinforced and casted for this test and as shown in **Fig.2**.

Details of the reinforcement provided in the beam are explained herein. In order to avoid the failure of the beams at torsional cracking load, each beam was designed to have a steel

reinforcement of 1.5% for the flexural reinforcement and 1% for transverse (stirrups) to the volume of the concrete. The ratio of the steel longitudinal and transverse reinforcement along with the geometrical and mechanical properties of the RC members influence the angle of the diagonal cracking, **Chalioris, and Karayannis, 2013**.

The percentage of reinforcements provided in the beam was slightly higher than the minimum required maintaining the integrity of the beam beyond cracking. Also this will represent the case of a deficient beam in terms of reinforcement, **MacGregor, and Ghoneim, 1995**.

All of beams are typical in cross-sectional dimensions ($b=100$ mm, $h=200$ mm) and have the same reinforcement as shown in **Fig.3** and were reinforced with 4 no. 10 mm bars in the longitudinal direction, ($A_s = 283$ mm²) and reinforced with closed stirrups in the transverse direction with 8 mm bars spaced at 100 mm on center, in the test region.

In RC torsional members, diagonal cracks are formed due to the same mechanism that is responsible for the formation of shear cracks. The diagonal tension cracks are found to be common in both shear and torsion. The main difference between shear cracking and torsional cracking lies in the crack pattern. Spiral-like crack pattern are found in torsional members, **Mitchell, and Collins, 1974, Hsu, 1984**.

2.4 Test Setup

The hydraulic testing machine was used to test all beams. The normal load can be applied by this machine on the specimen at several points and the supports should be remaining fixed against rotating around the longitudinal axis, i.e. twisting. In this research the applied loads outside the bed of the hydraulic testing machine are needed in order to obtain torsional movement.

The experimental requirements need to transmit the load from the center of the hydraulic testing machine to external points that represent load eccentricity so as the moment arm. The special clamping loading frame on each end of the beam used in this research is shown in **Fig.4**. This frame consists of two large steel clamps which work as arms for applied loadings with separated faces to connect them over the sample by large bolts; four bolts are used for each arm. This frame was fabricated of a hot-rolled structural steel angles which have a cross-sectional dimensions of L 1½" x 1½" x ¼" and L 1¼" x 1¼" x ⅜" and attached by welding. This final shape is similar to a bracket around external support and extended on one side to a distance of 600 mm. These arms were capable of providing a maximum eccentricity of 600 mm with respect to the longitudinal axis of the beam. In order to get pure torsion, the center of external support should coincide with the center of the moment arm.

An additional clamping was made at the mid-span of the testing beams which is made from 10 mm thick steel rods and 50 mm wide which were connected to mid-support as an intermediate confinement (twisting restraint).

In order to obtain pure torsion, a wide-flange structural steel girder with a depth of 250 mm and 3 m length is used to transmit the loads of the hydraulic testing machine to varied eccentricities from external supports. This girder was clamped to the hydraulic testing machine as shown in **Fig.5** and **Fig.6**. Reinforced concrete beams were tested under monotonically increasing torque up to



failure, the load was applied gradually. At each load increment 5kN, readings were acquired manually. The torque increased gradually up to failure of the beam.

In order to measure the absolute vertical displacement or AVD in brief, two dial gauges were attached at the bottom fibers at both end of the beams at a point 40 mm from the center of the longitudinal axis of the beams to measure the downward and upward displacement readings as shown in **Fig.4**. Then AVD is calculated according to Eq. (1). Angles of twist and the torsional moments were calculated from Eq. (2) and Eq. (3), respectively.

$$\delta = |y_1| + |y_2| \quad (1)$$

$$\theta = \tan^{-1} \delta/a \quad (2)$$

$$M_T = P \cdot x \quad (3)$$

where, (δ) is the absolute vertical displacement which is the summation of the readings of the absolute values two dial gauges multiplied by dial gauge factor which is 0.01, (y_1 and y_2) are the factored downward and upward displacement readings, respectively, (θ) is the angle of twist, (a) is the distance between dial gauges which have a fixed value of (80) mm, (M_T) is the torsional moments, (P) is the applied load and (x) is the eccentricity of loading.

3. TEST RESULTS AND DESCUSSION

Experimental test results for continuous beams B1, B2, B3 and B4 are shown in **Table9**. Variables considered in this experimental study were discussed herein.

3.1 Loading and Absolute Vertical Displacement

Fig.7 through **Fig.10** illustrate the relation between loadings and the absolute vertical displacement. Each figure has been gained from the average of the data of two beams which were tested under the same loading conditions. Four loading eccentricities were investigated with an increment of 10 cm in each stage. The loading eccentricities were 30, 40, 50 and 60 cm. The AVD was calculated by summing the absolute values of the adjacent gauges reading at each end multiplied by gauge reading factor.

The bar charts shown in **Fig.11** illustrate the recorded values of the 1st crack loading and failure loading for each case of load eccentricity. From the experimental test results and at failure loading stage; when the load eccentricity increased from 30cm to 60cm, the AVD increased by 11.27%, 32.1%, 46.92% for each 10 cm increment in eccentricity with reference to 30cm loading eccentricity, respectively. Also, it was found that each of the four beams behaved linearly under loading till first crack creation and then behaved non-linearly until failure. Also found from **Fig.11** that the load carrying capacity was decreased as the load eccentricity increased from 30cm to 60cm. The percentage of decrease in the load carrying capacity at failure stage were 22.07 %, 34.48 %, 49.65 % for each consecutive 10 cm increment in loading eccentricity with reference to 30cm loading eccentricity. This behavior obviously shows the major effect of load eccentricity so as the torsional moment on the beams.

3.2 Torsional Moments and Angle of Twist

The relation between torsional moments M_T and the angle of twist θ are shown in **Fig.12** through **Fig.15**. Each figure has been obtained from average of the data of two beams which were tested under the same loading conditions. For the four investigated loading eccentricity values, the torsional moments M_T and the angle of twist θ were calculated by Eq. (3) and (2), respectively. It was found that the torsional moments and at first cracking stage decreased as the load eccentricity increased from 30 cm to 60 cm. The percentages of decrease in the torsional moment values were 3.03 %, 9.09 %, 27.27 % for the each consecutive 10 cm increments in loading eccentricity with reference to 30cm loading eccentricity. This is demonstrated in the bar chart shown in **Fig. 16**.

At failure loading stage, the torsional moment of the beams undergoes increases in relatively high percentage and then under large eccentricity of loading values, the increasing rate was very slightly in comparison with low loading eccentricity value. The percentage of increasing in the torsional moments were 3.91%, 9.2%, 0.69% for each 10 cm increment in loading eccentricity with reference to 30cm loading eccentricity. This behavior is very clear as the relation between torsional moments M_T and loading eccentricities are directly proportional with reference to the decreasing of failure loading for each case as explained previously.

3.3 Continuous Reinforced Concrete Beams Behavior at First Cracking Stage

The behavior of the beams at first cracking stage under all loading eccentricities values is shown in the **Fig. 16**. It was found that at low load eccentricity value, beams were twisted much more than larger eccentricities values before the 1st cracking. So when the loading eccentricity values twice experimentally from 30 cm to 60 cm, the generated angle of twist under 30cm eccentricity was 158.41% times the generated angle of twist at 60 cm eccentricity. This behavior was due to the higher values of loading at low loading eccentricities which will induce greater values of AVD (before first cracking occur) as the angle of twist is directly proportional to AVD according to Eq. (2) as listed previously.

On the other hand, and at the failure stages; twisting of beams is seen to be increased as the load eccentricity values increased as shown in **Fig. 17**. The percentage of increasing in the angle of twist were 17.95%, 31.43%, 45.76% for each consecutive 10 cm increment in loading eccentricity with reference to 30cm loading eccentricity. The relation between the torsional moments M_T and the angle of twist θ still directly proportional but it changed to non-linear behavior.

4. CONCLUSIONS AND RECOMMENDATIONS

4.1. Conclusions

According to experimental results reported previously, the following conclusions are presented:

1. All of the tested RC beams cracked under pure torsion in a similar pattern.
2. The generated cracks in RC beams due to twisting were close especially near to external supports, i.e. near to points of eccentric applied loads.
3. The cracks in RC beams with large loading eccentricity values (50 cm and 60 cm) were limited to 2/3 of each span length (1m) as they start from each external support and vanish at the last 1/3 beams span.



4. The cracks in RC beams under low loading eccentricity values (30 cm and 40 cm) were extended to mid-support and met the cracks generated in the adjacent span forming a spiral cracks along beams.

4.2. Recommendations

The following research on RC continuous beams under pure torsions is recommended for future research work:

1. Investigating the torsional behaviour of different grades of concrete such as high strength and ultra high strength.
2. Retrofitting RC beams with carbon fibre reinforced polymers (CFRP) fabrics and laminates and retesting.
3. Investigating RC beams elongation under pure torsion.
4. Investigating the behaviour of RC beams under pure torsion by modelling of material properties in finite elements and nonlinear solution techniques.

REFERENCES

- American Concrete Institute ACI, 1997, *Standard Practice for Selecting Proportions for Normal, Heavy Weight and Mass Concrete*, ACI 211.1-91 (Re-approved 2002), ACI Manual of Concrete Practice.
- American Society for Testing Materials ASTM, 2002, *Standard Specification for Deformed and Plain Billet-Steel Bars for Concrete Reinforcement*, A 615/A 615M-01, Annual Book of ASTM.
- Central Organization of Standardizations and Quality Control, 1984, *Portland Cement*, Iraqi Standard No. 5.
- Central Organization of Standardizations and Quality Control, 1984, *Natural Aggregate used In Concrete and Construction*, Iraqi Standard No. 45.
- Chalioris, C. E., and Karayannis, C. G., 2013, *Experimental investigation of RC beams with rectangular spiral reinforcement in torsion*, Journal of Engineering Structures, Vol. 56, PP. 286-297.
- Fanella, D. A. and Rabbat, B.G., 1997, *Design of Concrete Beams for Torsion*, Engineering Bulletin EB106.02D, Portland Cement Association, Skokie, III.
- Hsu, T. T. C., 1968, *Torsion of Structural Concrete - Behaviour of Reinforced Concrete Rectangular Members*, Torsion of Structural Concrete, ACI Special Publication, SP-18, Vol. 11, No. 31, PP. 261-306.
- Hsu, T.T.C., 1984, *Torsion of Reinforced Concrete*, Van Nostrand Reinhold, Inc., New York, N.Y., 516 pages.



- Kamara, M. E. and Rabbat B. G., 2005, *Notes on ACI 318- 05 Building Code Requirements for Structural Concrete with Design Applications*, Portland Cement Association, EB705.
- Kamara, M. E. and Rabbat B. G., 2007, *Torsion Design of Structural Concrete Based on ACI 318-0*, Professional development series of Portland Cement Association PCA, Special Advertising Section.
- Kumar, C.A., Mohan, M., Rajesh, D. V. and Kulkarni, P., 2015, *Behavior of Fiber Reinforce Concrete Beam in Pure Torsion*, International Journal of Research in Engineering and Technology, Vol. 4, No. 5, PP. 551-556
- MacGregor, J. G. and Ghoneim, M. G., 1995, *Design for Torsion*, ACI Structural Journal, Vol. 92, No. 2, PP. 211-218.
- McCormac J. C. and Brown R. H., 2014, *Design of Reinforced Concrete*, John Wiley & Sons, Inc, Ninth edition.
- Mahmoud E. K., and Basile G. R., 2007, *Torsion Design of Structural Concrete Based on ACI 318-05*, Portland Cement Association, Professional Development Hours - Structural Engineer.
- Mitchell, D. and Collins, M.P., 1974, *Diagonal Compression Field Theory – A Rational Model for Structural Concrete in Pure Torsion*, Structural Journal of the American Concrete Institute, Vol. 71, No. 8, PP. 396-408.

NOMENCLATURE

a= distance between adjacent dial gage, mm.

M_T = torsional moments, kN.m.

P = applied load, kN.

x = eccentricity of loading, m.

y_1, y_2 = factored upward and downward displacement, mm.

δ = absolute vertical displacement, mm.

θ = angle of twist.

**Table 1.** Chemical properties of cement* used throughout this work.

Oxide Composition	Abbreviation	Percentage by Weight	Limit of Iraqi Specification NO.5/1984
Lime	CaO	63.23	–
Silica	SiO ₂	20.12	–
Alumina	Al ₂ O ₃	5.54	–
Iron Oxide	Fe ₂ O ₃	3.41	–
Sulphate	SO ₃	1.61	≤ 2.8 %
Magnesia	MgO	4.75	≤ 5.0 %
Potash	K ₂ O	0.36	–
Soda	Na ₂ O	0.2	–
Loss on ignition	L. O. I.	0.73	≤ 4.0 %
Insoluble residue	I. R.	1.24	≤ 1.5 %
Main Compounds (Bogue's Equations)			
Tricalcium Silicate	C ₃ S	57.74	–
Dicalcium Silicate	C ₂ S	14..21	–
Tricalcium Aluminate	C ₃ A	8.92	–
TetracalciumAlumino- Ferrite	C ₄ AF	10.34	–

*These chemical tests were carried out in the lab of Central Organization for Standardization and Quality Control.

Table2. Physical properties of cement* used throughout this work.

Physical Properties	Test Results	Limits of Iraqi Specification NO.5/1984
Specific surface area (Blaine method) (m ² /kg)	325	≥ 230
Soundness (Le-chatelier method) (mm)	0.66	<10
Setting time (Vicat's method)		
Initial setting (hrs:min.)	2:40	≥ 45 min.
Final setting (hrs:min.)	4:25	≤ 10 hrs
Compressive strength (MPa)		
3 days	18.90	≥ 15
7 days	28.70	≥ 23

*These physical tests were carried out in the lab of Central Organization for Standardization and Quality Control.

**Table 3.** Grading of fine aggregate

Sieve Size (mm)	Cumulative Passing (%)	Limits of the Iraqi Specification No.45/1984, Zone 3
10	100	100
4.75	92.6	90-100
2.36	87.3	85-100
1.18	77.9	75-100
0.60	63.1	60-79
0.30	28.5	12-40
0.15	7.4	0-10
Fineness modulus =2.43		

Table 4. Physical properties of fine aggregate

Physical Properties	Test Results	Limits of the Iraqi Specification No.45/1984
Specific gravity	2.65	-
Sulfate content %	0.2	≤ 0.5 %
Absorption %	0.70	-

Table 5. Grading of coarse aggregate

Sieve Size (mm)	Cumulative Passing (%)	Limitations of the Iraqi Specification No.45/1984
20.0	100	95-100
14.0	-	-
10.0	59	30-60
5.00	1	0-10
2.36	-	-

Table 6. Physical properties of coarse aggregate

Physical Properties	Test Result	Limit of Iraqi Specification No. 45/1984
Specific gravity	2.63	-
Sulfate content %	0.06	≤ 0.1 %
Absorption %	0.63	-

Table 7. Properties of steel reinforcement

Nominal Diameter (mm)	Measured Diameter (mm)	Modulus of Elasticity (Es) (GPa)	Yield Stress (fy) (MPa)	Ultimate Stress (fu) (MPa)
8	7.18	200	430	602
10	9.53	200	484	719

Table 8. Proportions of constituents of concrete mix

Parameter	Normal Strength Concrete Properties
Water/cement ratio	0.4
Water (kg/m ³)	156
Cement (kg/m ³)	390
Fine aggregate (kg/m ³)	585
Coarse aggregate (kg/m ³)	1170
Density (kg/m ³)	2577

Table 9. Experimental test results of test beams

Test Beams	Loading Eccentricity, m	Loading, kN		Torsional Moment capacity, kN.m	Absolute Vertical Displacement, mm		Angle of Twisting, degree	
		at First Cracking Stages	at Failure Stages		External Support 1	External Support 2	External Support 1	External Support 2
B1	0.3	55	72.5	21.75	11.5	11.71	8.18	8.33
B2	0.4	40	56.5	22.6	13.58	13.87	9.63	9.84
B3	0.5	30	47.5	23.75	15.26	15.4	10.82	10.89
B4	0.6	20	36.5	21.9	16.97	17.13	11.98	12.08

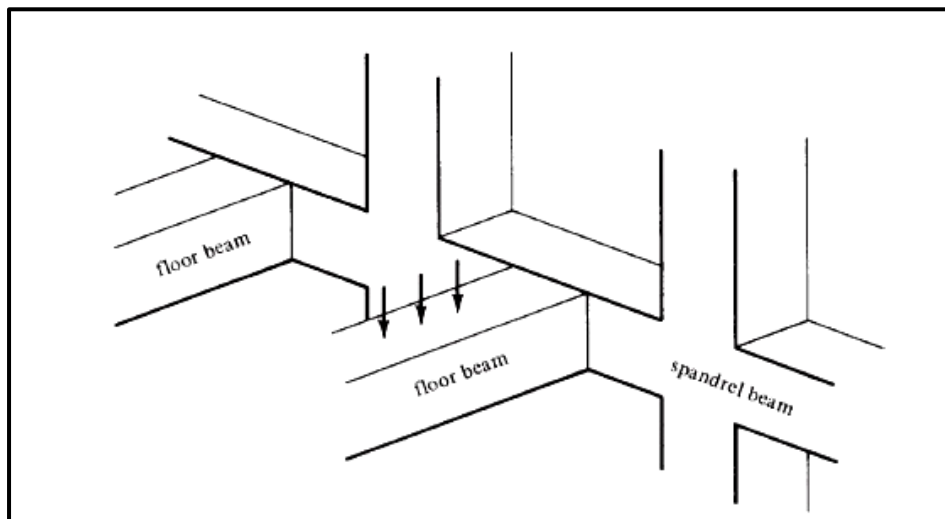


Figure 1. Torsion in spandrel beams.



Figure 2. Reinforced concrete test beams.

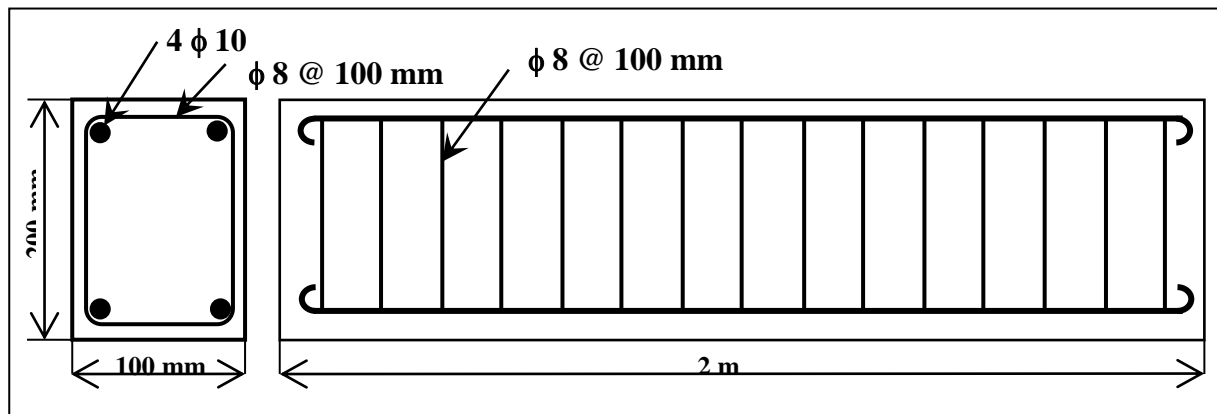


Figure 3. Reinforcement details for test beams.

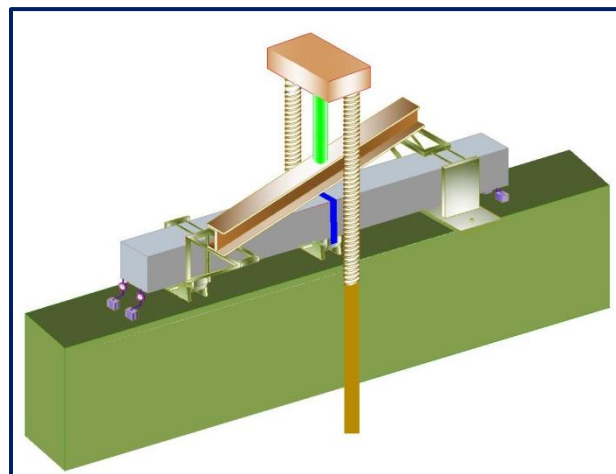


Figure 4. Test Setup.



Figure 5. Special clamping torsional frame



Figure 6. Steel girder fixed to testing machine

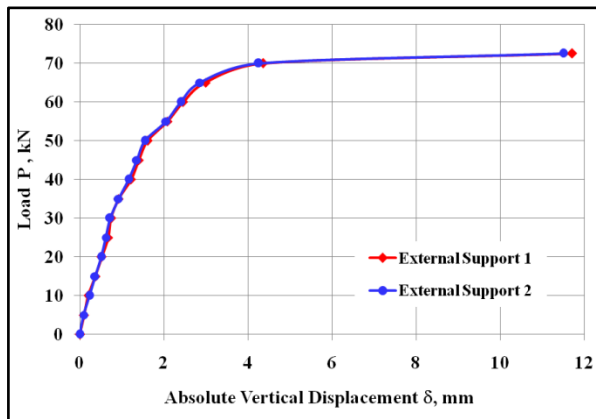


Figure 7. Variation of the 30-cm eccentricity load with the absolute vertical displacement

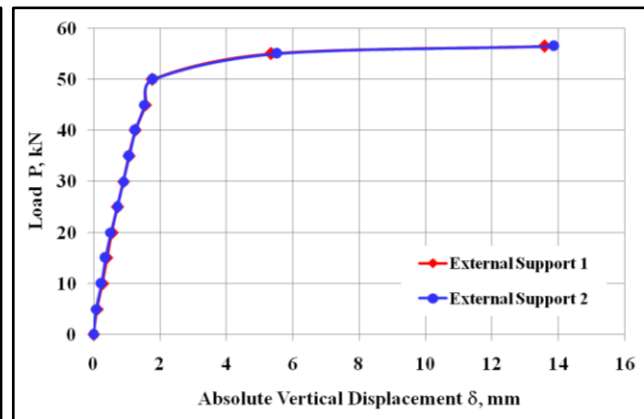


Figure 8. Variation of the 40-cm eccentricity load with the absolute vertical displacement

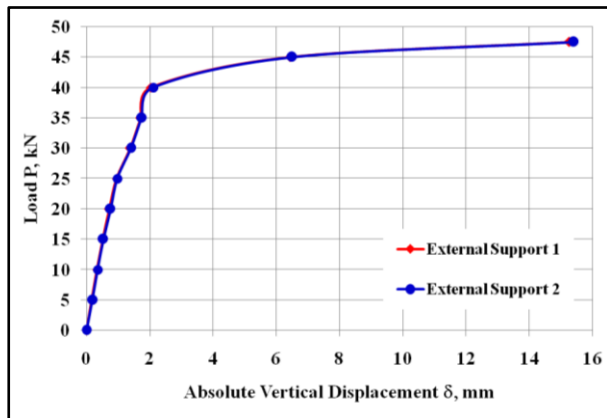


Figure 9. Variation of the 50-cm eccentricity load with the absolute vertical displacement

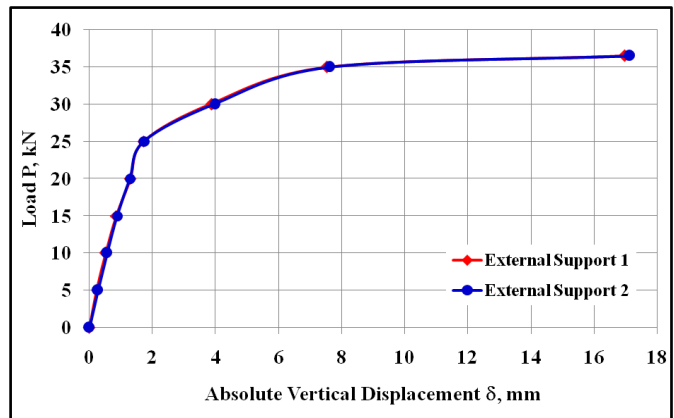


Figure 10. Variation of the 60-cm eccentricity load with the absolute vertical displacement

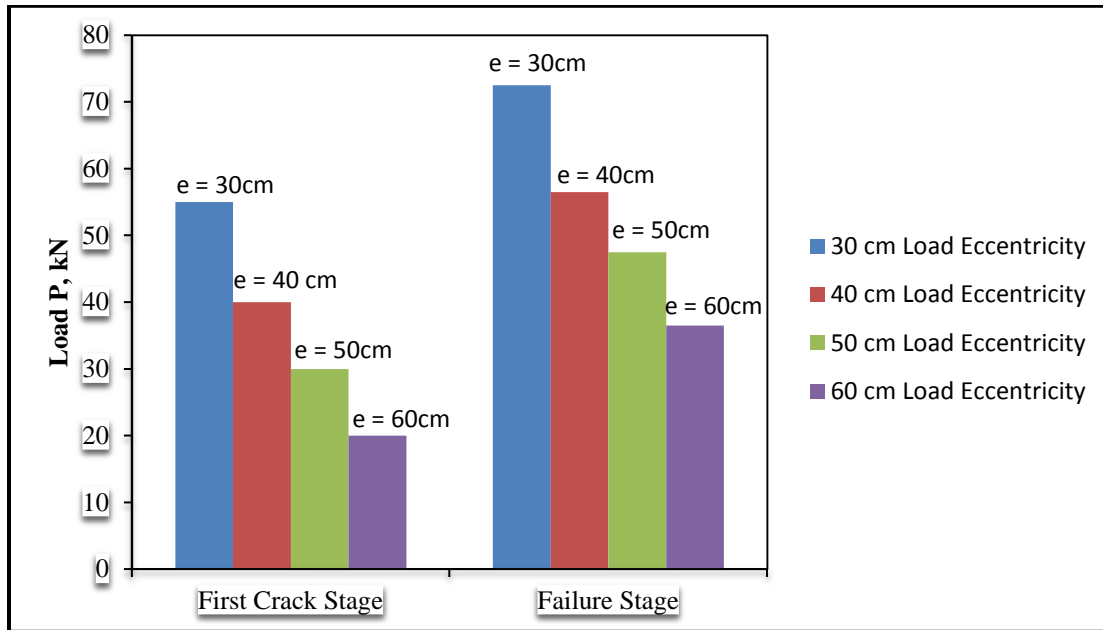


Figure 11. Loadcarrying capacity of beams at 1st cracking and failure stages

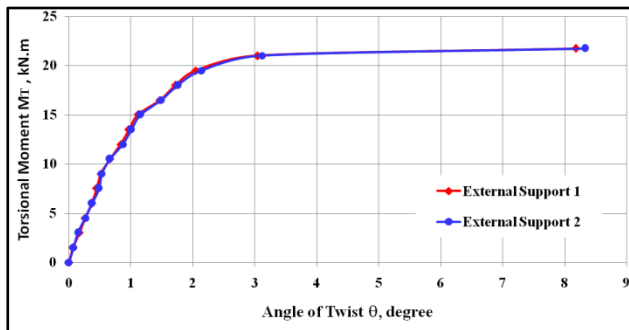


Figure 12. Variation of torsional moment vs. angle twist for 30 cm loading eccentricity

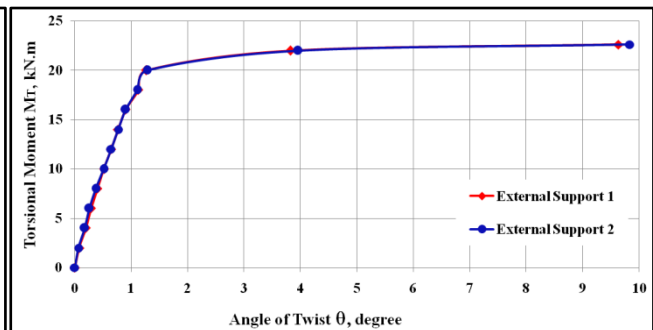


Figure 13. Variation of torsional moment vs. angle twist for 40 cm loading eccentricity

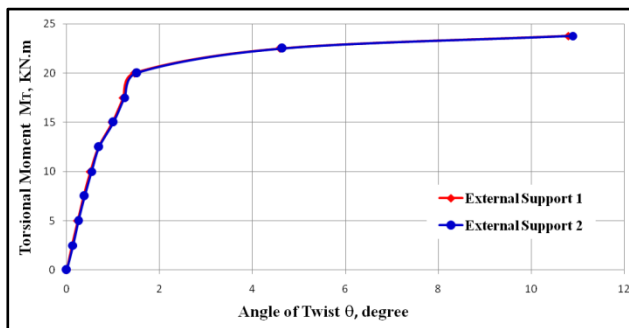


Figure 14. Variation of torsional moment vs. angle twist for 50 cm loading eccentricity

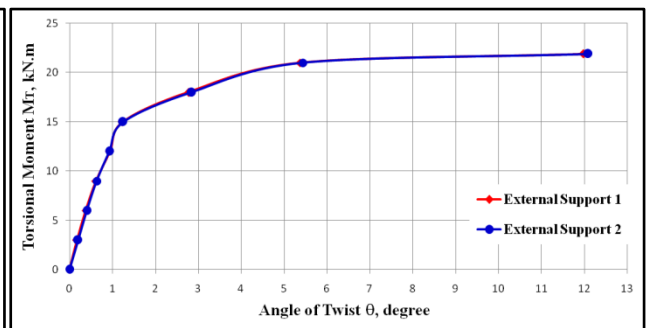


Figure 15. Variation of torsional moment vs. angle twist for 60 cm loading eccentricity

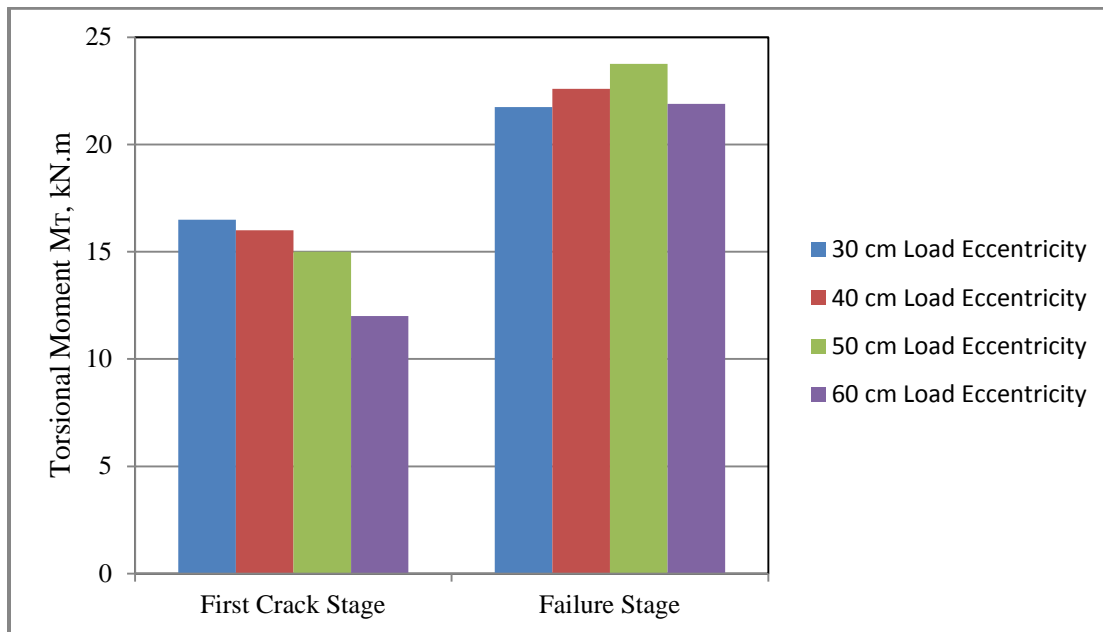


Figure 16. Torsional moment variation at 1st cracking and failure stages.

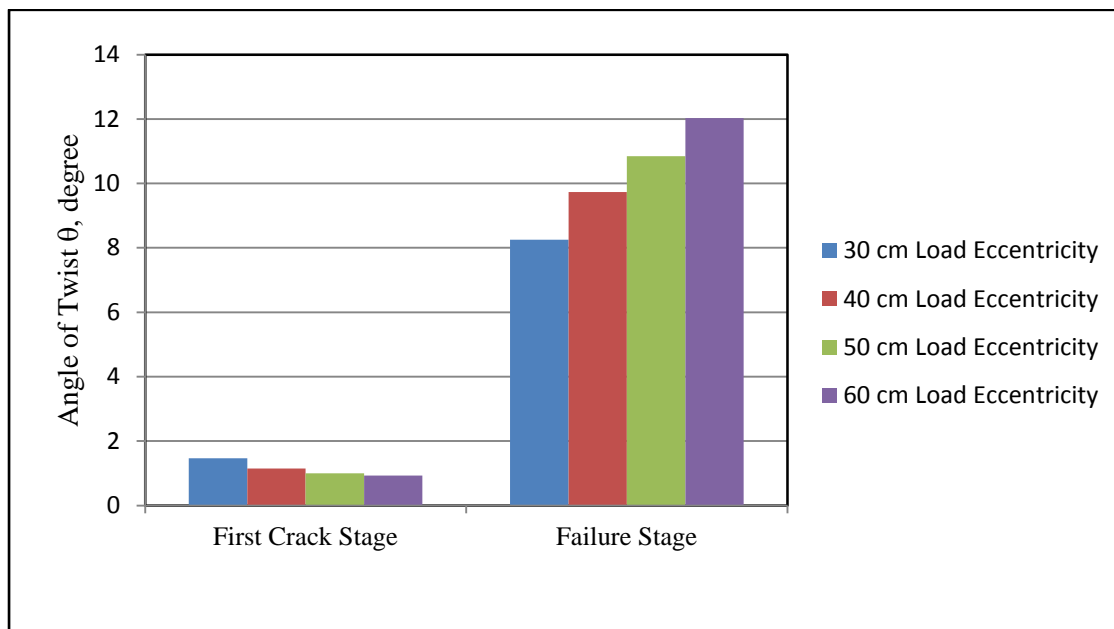


Figure 17. Angle of twisting variation at 1st cracking and failure stages